Bulgarian Journal of Physics vol. **46** (2019) 445–454

Ab initio Rotation in ^{10}Be

M.A. Caprio[1], **P.J. Fasano**[1], **A.E. McCoy**[2], **P. Maris**[3], **J.P. Vary**[3]
[1]Department of Physics, University of Notre Dame, Notre Dame, Indiana 46556-5670, USA
[2]TRIUMF, Vancouver, British Columbia V6T 2A3, Canada
[3]Department of Physics and Astronomy, Iowa State University, Ames, Iowa 50011-3160, USA

Received *9 December 2019*

Abstract. *Ab initio* theory describes nuclei from a fully microscopic formulation, with no presupposition of collective degrees of freedom, yet signatures of clustering and rotation nonetheless arise. We can therefore look to *ab initio* theory for an understanding of the nature of these emergent phenomena. To probe the nature of rotation in ^{10}Be, we examine the predicted rotational spectroscopy from no-core configuration interaction (NCCI) calculations with the Daejeon16 internucleon interaction, and find spectra suggestive of coexisting rotational structures having qualitatively different intrinsic deformations: one triaxial and the other with large axial deformation arising primarily from the neutrons.

KEY WORDS: *Ab initio* nuclear theory, no-core configuration interaction (NCCI) approach, nuclear rotation, Daejeon16 interaction

1 Introduction

Ab initio nuclear theory attempts to provide a fully microscopic and predictive theory of nuclei, by solving the quantum many-body problem for the nucleons and their free-space interactions. Indications of collective phenomena, including both clustering [1–5] and rotation [6–8], may be found in the results of *ab initio* calculations.

From their *ab initio* microscopic description, we may seek not only quantitative predictions, but also qualitative insight into the structure of these collective degrees of freedom. *Ab initio* calculations provide access to an extensive set of observables, such as transition strengths, for identifying collective excitations. The calculated spectroscopy can go far beyond what is in practice experimentally accessible for the collective states of these light nuclei, thereby making collective patterns easier to identify. Furthermore, the calculated wave functions can be analyzed as a more direct probe of the nature of their collective structure [9–12].

For the odd-mass Be isotopes ^{7,9,11}Be, the nature of *ab initio* emergent rotation has been probed through such approaches in Ref. [12], based on no-core configuration interaction (NCCI) [13] [or no-core shell model (NCSM)] calculations with the Daejeon16 internucleon interaction [14]. In the present contribution, we turn to the even-mass isotope ^{10}Be, which is experimentally known to have a rich rotational spectroscopy [15] and has been suggested to exhibit proton-neutron triaxiality [16]. After commenting on the experimental situation and interpretations for rotational bands in ^{10}Be (Sec. 2), we examine the *ab initio* calculated rotational spectroscopy and the oscillator structure of the resulting wave functions (Sec. 3).

2 Background: Experiment and Cluster Molecular Interpretation

In ^{10}Be, the low-lying, positive-parity spectrum is known experimentally to contain two $K^P = 0^+$ bands: the ground state band and an excited band at $6.2\,\mathrm{MeV}$ [17–19]. Both bands are observed up to their 4^+ members.[1] The two bands have significantly different moments of inertia, based on the observed band member energies [$E(J) = E_0 + AJ(J+1)$]:[2] the excited band has a slope ($A \approx 0.20\,\mathrm{MeV}$) lower than that of the ground state band ($A \approx 0.59\,\mathrm{MeV}$) by about a factor of 3, indicating approximately thrice the moment of inertia. With its shallower slope, the excited band becomes yrast at $J = 4$.

Microscopic antisymmetrized molecular dynamics (AMD) calculations [22–24] support an interpretation in which ^{10}Be may be described as a molecule consisting of two α clusters (essentially an ^{8}Be core) plus two "valence" neutrons which occupy molecular orbitals around these clusters. In the ground state band, these two neutrons occupy π orbitals (that is, with angular momentum projection ± 1 along the molecular axis), loosely corresponding to a spherical shell model $0\hbar\omega$ configuration. In the excited band, these two neutrons occupy σ orbitals (that is, with angular momentum projection 0 along the molecular axis), loosely corresponding to a spherical shell model $2\hbar\omega$ configuration. This configuration yields a larger moment of inertia, due both to the greater spatial extent of the neutron orbitals themselves along the molecular axis, and to an accompanying increase in the inter-α separation [23].

[1] The experimental band members for the $K^P = 0_1^+$ band are 0_1^+ ($0.00\,\mathrm{MeV}$), 2_1^+ ($3.37\,\mathrm{MeV}$), and 4_2^+ ($11.76\,\mathrm{MeV}$), which was assigned as (4^+) in Ref. [20] but confirmed as 4^+ in Ref. [18]. Those for the $K^P = 0_2^+$ band are 0_2^+ ($6.18\,\mathrm{MeV}$), 2_3^+ ($7.54\,\mathrm{MeV}$), and 4_1^+ ($10.15\,\mathrm{MeV}$), which was assigned as 3^- in Ref. [20] but revised to 4^+ in Refs. [17,19]. Furthermore, Ref. [18] identifies a putative $K^P = 2^+$ band, consisting of 2_2^+ ($5.96\,\mathrm{MeV}$) and 3_1^+ ($9.4\,\mathrm{MeV}$), where this latter level is newly identified with assignment (3^+) in Ref. [18].

[2] Rotational band members built on an axially symmetric intrinsic state $|\phi_K\rangle$, with projection K of the angular momentum onto the intrinsic symmetry axis, have angular momenta $J \geq K$, with energies $E(J) = E_0 + AJ(J+1)$, where the rotational energy constant $A \equiv \hbar^2/(2\mathcal{J})$ is inversely related to the moment of inertia $\mathcal{J}$, and $E_0 = E_K - AK^2$ is related to the energy E_K of the rotational intrinsic state [21].

Furthermore, the AMD calculations suggest that the ground state of this nucleus has triaxial deformation [22, 24], specifically, proton-neutron triaxiality arising from the combination of an overall prolate distribution for the protons and an overall oblate distribution of neutrons, which are then oriented relative to each other such as to give an overall triaxial shape.

In ideal triaxial rotation of an even-even nucleus, a more complex rotational spectrum is expected [25, 26], in which the $K = 0$ ground state band is accompanied by $K = 2, 4, \ldots$ bands, with $E2$ connections. Indeed, the AMD calculations predict that a $K = 2$ side band should accompany the ground state band of ^{10}Be [23]. A possible (very short) experimental side band has been proposed [18], consisting of the experimental 2^+ state at $5.96\,\mathrm{MeV}$ and a tentatively identified 3^+ member. The resulting slope parameter ($A \approx 0.57\,\mathrm{MeV}$) is essentially identical to that of the ground state band.

3 *Ab initio* Rotational Spectrum

In the NCCI approach, the nuclear many-body Hamiltonian is represented in terms of a basis of antisymmetrized products (Slater determinants) of single-particle states, typically harmonic oscillator states, and then diagonalized to yield the energies and wave functions. Any actual calculation must be carried out using a finite, truncated basis, *e.g.*, restricted to at most $N_{\max}$ quanta of excitation above the lowest Pauli-allowed filling of oscillator shells.

The excitation spectrum for the positive-parity states of ^{10}Be, as obtained in an NCCI calculation with the Daejeon16 internucleon interaction,[1] is shown in Figure 1. The calculated levels (squares) are overlaid with the experimental levels (horizontal lines) [17–20], and energies are plotted against angular momentum scaled as $J(J+1)$ to facilitate recognizing rotational bands. These calculations, obtained using the M-scheme NCCI code MFDn [28–30], are obtained using a harmonic oscillator basis with oscillator scale parameter $\hbar\omega = 15\,\mathrm{MeV}$ and truncation $N_{\max} = 12$.

The energies and wave functions obtained in any such truncated calculation provide only an approximation to the true solution which would be obtained in the full many-body space. These results may be expected to converge towards the full-space results with increasing $N_{\max}$, but different aspects of the calculated spectroscopy can have very different sensitivities, both to the oscillator basis parameter $\hbar\omega$ and to $N_{\max}$ itself, as illustrated in Figure 2.

For instance, the calculated *energy eigenvalues* themselves are changing on a scale of MeV with each step in $N_{\max}$ [Figure 2(a)], while many *excitation en-*

[1] The Daejeon16 internucleon interaction [14] is obtained starting from the Entem-Machleidt chiral perturbation theory interaction [27], which is then softened via a similarity renormalization group transformation and adjusted via a phase-shift equivalent transformation to yield an accurate description of light nuclei with $A \leq 16$.

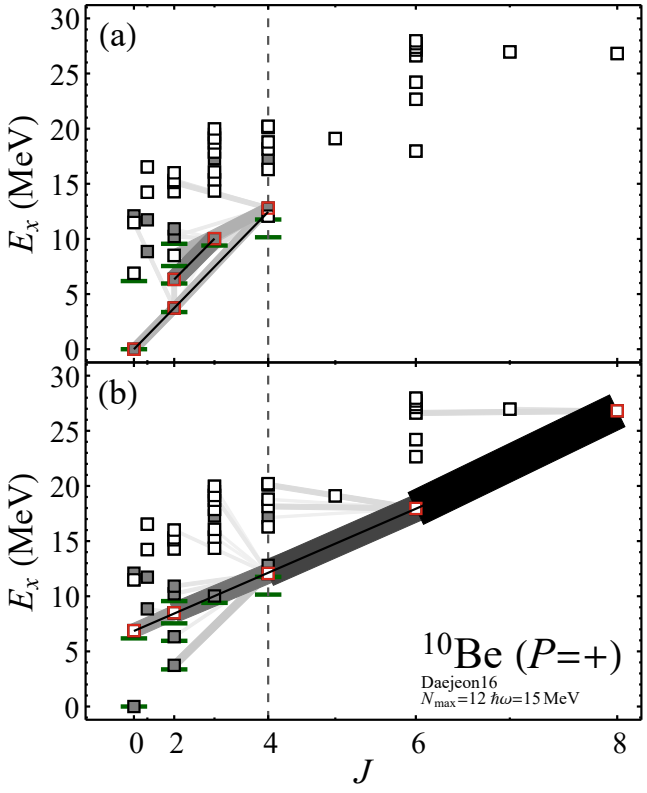

Figure 1. *Ab initio* calculated energy spectrum for ^{10}Be positive parity, showing $E2$ transitions originating from members of rotational bands: (a) the ground state band ($K^P = 0^+$) and side band ($K^P = 2^+$) and (b) the long band ($K^P = 0^+$). Rotational band members are highlighted (red squares), and rotational energy fits are indicated by lines. Experimental energies (green horizontal lines) are shown for comparison. States are approximately classified as $0\hbar\omega$ (filled symbols) or $2\hbar\omega$ (open symbols). The J-decreasing $E2$ transitions originating from the rotational band members are shown (specifically, transitions with $J_f < J_i$ or with $J_f = J_i$ and $E_f < E_i$), with line thickness proportional to the $B(E2)$ strength. The maximal angular momentum possible in the $0\hbar\omega$ valence space is indicated by the vertical dashed line. Calculation obtained for the Daejeon16 interaction, with oscillator basis parameter $\hbar\omega = 15\,\mathrm{MeV}$ and truncation $N_{\max} = 12$.

ergies (or relative energies, in general) are much better converged [Figure 2(b)], on a scale of tens of keV. Similarly, individual calculated $E2$ strengths do not typically approach a stable, converged value in the computationally accessible spaces [Figure 2(c)], yet many calculated relative transition strengths, especially among members of the same rotational band or bands with related structure, are much more stable [Figure 2(d)]. Thus, even when individual energies and

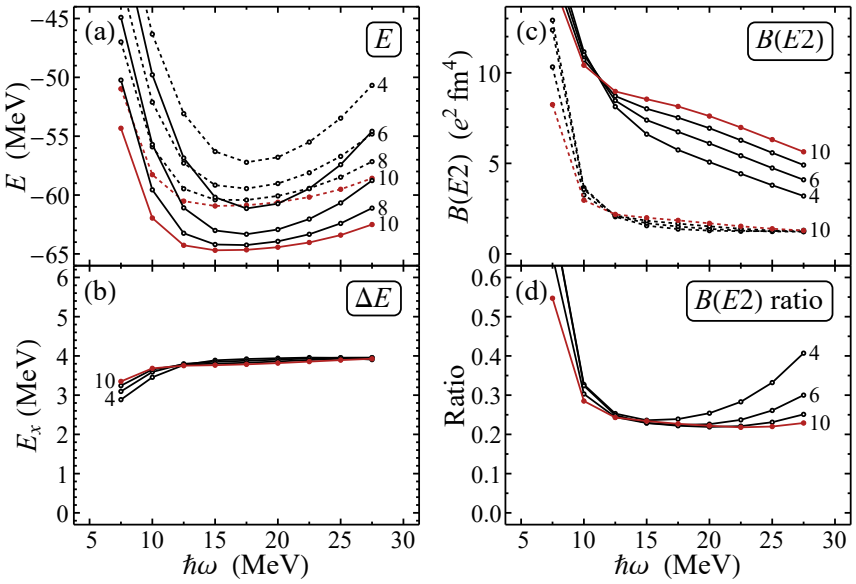

Figure 2. Convergence of calculated energy and transition observables for ^{10}Be (top) and corresponding relative observables (bottom): (a) energies of the 0^+_1 ground state (solid curves) and 2^+_1 rotational band member (dashed curves), (b) the energy difference $E(2^+_1) - E(0^+_1)$, (c) transition strengths $B(E2; 2^+_1 \to 0^+_1)$ (solid curves) and $B(E2; 2^+_2 \to 2^+_1)$ (dashed curves) within the ground state rotational band and between the side band and the ground state band, respectively, (d) the transition strength ratio $B(E2; 2^+_2 \to 2^+_1)/B(E2; 2^+_1 \to 0^+_1)$. Calculated values are shown as functions of the basis parameter $\hbar\omega$, for $N_{\max} = 4$ to 10 (as labeled).

transition strengths are not yet well converged, rotational patterns involving relative energies and transition strengths within bands are readily recognized (see discussions in Refs. [8, 12, 31]).

Returning to the calculated positive-parity spectrum for ^{10}Be in Figure 1, we may observe that the near-yrast states form three rotational bands, in rough correspondence to the three experimental bands (Sec. 2). A $K^P = 0^+$ ground state band (0^+, 2^+, 4^+) is readily recognized in the calculations, from the rotational energies [linear in $J(J+1)$] and enhanced $E2$ transitions [Figure 1(a)]. The moment of inertia ($A \approx 0.62$ MeV) is consistent with experiment. The terminating angular momentum ($J = 4$) is also the maximal angular momentum which can be constructed for ^{10}Be in the p-shell valence space (or $0\hbar\omega$ space).

Then, the calculated yrare 2^+ state and the first 3^+ state are connected by a strong $E2$ transition [Figure 1(a)]. There are also significant $E2$ strengths from these states to the ground state band. These states thus form a putative short $K^P = 2^+$ band, a "side band" (spectroscopically speaking) to the ground state

band. The calculated band head is at just over $6\,\mathrm{MeV}$ excitation energy, while the energy difference gives a moment of inertia ($A \approx 0.62\,\mathrm{MeV}$) essentially identical to that of the ground state band.

The enhanced transitions between the side band and ground state band are, specifically, the $2^+_{K=2} \to 2^+_{K=0}$ and $3^+_{K=2} \to 4^+_{K=0}$ transition. This transition pattern is not at all what would be expected from the Alaga rules [32] for transitions between true $K = 2$ and $K = 0$ bands, as obtained for an axially symmetric rotor. For instance, the $2_{K=2} \to 2_{K=0}$ and $2_{K=2} \to 0_{K=0}$ transitions should be of comparable strength [$B(E2; 2_{K=2} \to 2_{K=0})/B(E2; 2_{K=2} \to 0_{K=0}) \approx 1.4$] for an axially symmetric rotor, while the computed $2^+_{K=2} \to 0^+_{K=0}$ strength here is negligible. Rather, the calculated transitions follow the γ-parity [33] selection rules expected for a $\gamma = 30^\circ$ triaxial rotor (see, *e.g.*, Figure 17 of Ref. [34]), where only states of opposite γ parity are connected by $E2$ transitions.

Finally, an excited $K^P = 0^+$ band starts from the calculated 0^+_2 state as its band head [Figure 1(b)] and extends through an 8^+ member. The excited band members have essentially negligible $E2$ connections to the ground state band members. (An exception arises since the 4^+ members of the ground and excited $K^P = 0^+$ bands undergo transient two-state mixing, when their calculated energies cross at $N_{\mathrm{max}} = 10$ and 12, as discussed below. This mixing gives rise to modest transitions connecting the 4^+ and 2^+ members of the different bands, seen in Figure 1.)

The excited $K^P = 0^+$ band has a much shallower slope ($A \approx 0.26\,\mathrm{MeV}$), and thus larger moment of inertia, than the ground state band, as in experiment. This larger deformation is already suggested by the greater in-band $E2$ strengths [comparing Figure 1(a) and Figure 1(b)]. However, $E2$ observables are only partially sensitive to this deformation, as it appears to largely arise from the neutrons. Comparing the calculated quadrupole moment of the proton distribution (*i.e.*, the physical electric quadrupole moment) with that of the neutron distribution gives a ratio of merely $Q_n/Q_p \approx 0.7$ for the ground state band, but a much larger ratio $Q_n/Q_p \approx 2.1$ for the excited $K^P = 0^+$ band (see also Figure 18 of Ref. [7]).

Before attempting any meaningful comparison with experiment, we must take into account the convergence of the calculated energies of the band members, as explored for $N_{\mathrm{max}} = 6$ to 12 in Figure 3. Within the ground state band, the excitation energies have minimal N_{max} dependence, although the slope does slightly decrease (from $A \approx 0.64\,\mathrm{MeV}$ to $0.62\,\mathrm{MeV}$) over this range of N_{max}. The side band descends in excitation energy by $\lesssim 1\,\mathrm{MeV}$, indeed, moving closer to experiment [Figure 1(a)]. In contrast, the calculated excitation energies of the excited $K^P = 0^+$ band members plummet by more than $5\,\mathrm{MeV}$. The ground state and excited band 4^+ members cross, so that the excited band 4^+ member becomes yrast, as in experiment, at $N_{\mathrm{max}} = 12$. The calculated excited band

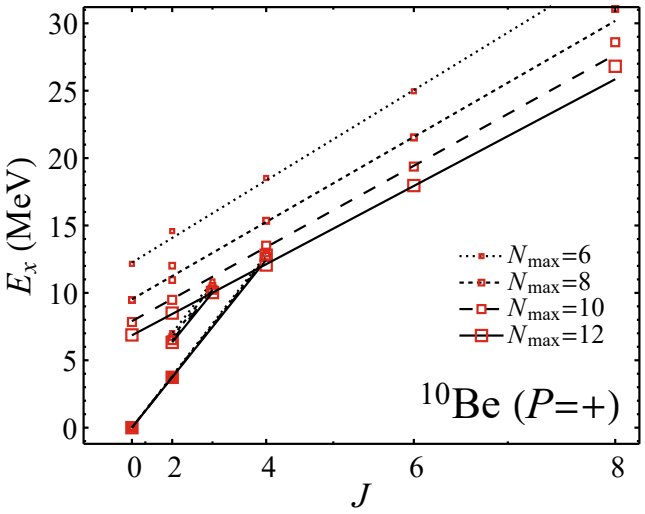

Figure 3. Calculated excitation energies for rotational band members in ^{10}Be, for $N_{\max} = 6$ to 12 (dotted through solid curves).

members at $N_{\max} = 12$ still lie above experiment, by $\sim 0.7\,\mathrm{MeV}$ for the band head and $\sim 2\,\mathrm{MeV}$ for the 4^+ member [Figure 1(b)].

In a conventional shell-model description, based on interacting nucleons in a harmonic-oscillator mean-field potential, there is a natural organization of states into $0\hbar\omega$ and $2\hbar\omega$ states based on the predominant number of oscillator excitations above the valence shell. Such a classification seems to also be relevant to nuclear states obtained in *ab initio* approaches, despite there being no explicitly imposed mean field.

In particular, the decomposition of the calculated wave function into the contributions coming from oscillator basis configurations with different numbers of oscillator quanta (*e.g.*, Ref. [35]) can be suggestive of a $0\hbar\omega$ or $2\hbar\omega$ nature, though this interpretation is at best approximate (see Ref. [12] for discussion). To explore the oscillator structure of the ^{10}Be rotational bands, let us examine such decompositions, that is, by the number N_{ex} of excitation quanta relative to the lowest Pauli allowed oscillator configuration, as shown in Figure 4 for the $K^P = 0^+$ band head states.

The predominant contribution to the ground state comes from $N_{\mathrm{ex}} = 0$ (or $0\hbar\omega$) configurations [Figure 4(a)]. Similar decompositions are found for the other members of the ground state band and side band, suggesting that their essential structure can largely be described in a $0\hbar\omega$ shell model.

In contrast, the excited $K^P = 0^+$ band could not possibly be explained entirely within the $0\hbar\omega$ shell model, as we may recall it extends beyond the maximal valence angular momentum ($J = 4$). For the excited 0^+ band head [Figure 4(b)],

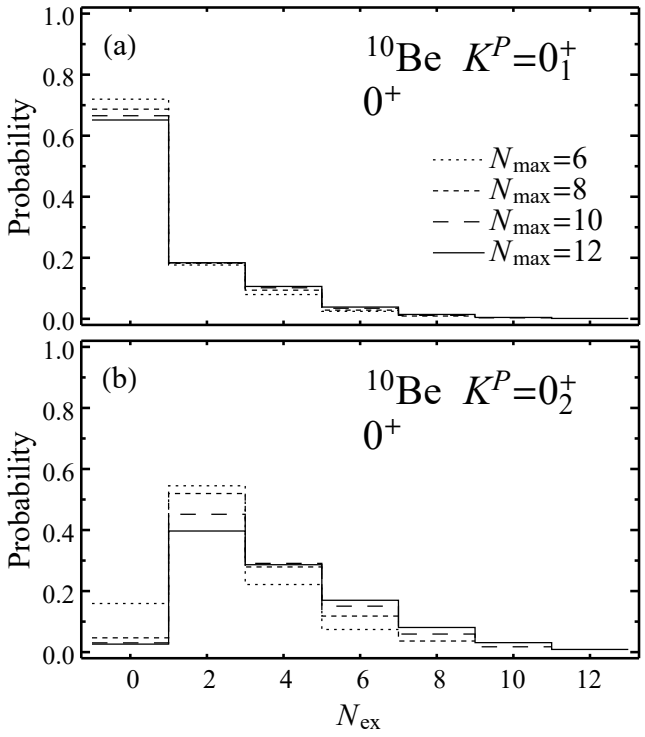

Figure 4. Decompositions of ^{10}Be rotational band heads in oscillator space: (a) the 0^+ ground state and (b) the 0^+ band head of the long band. Shown for $N_{max} = 6$ to 12 (dotted through solid curves).

the predominant contributions come from $N_{ex} = 2$ ($2\hbar\omega$) and higher configurations, falling off gradually with higher N_{ex}, while the $N_{ex} = 0$ contribution is just a few percent. Similar decompositions are found for the other excited $K^P = 0^+$ band members.

4 Conclusion

Ab initio NCCI calculations of ^{10}Be were already known to be suggestive of rotational structure [6,7]. However, the present calculations with the Daejeon16 interaction provide a picture which is qualitatively and, to within the limitations of convergence, quantitatively consistent with experiment and which would seem to be qualitatively consistent with the expectations from microscopic cluster molecular descriptions as well.

Two coexisting rotational structures are found at low energy in the ^{10}Be positive parity space. The ground state band ($K^P = 0^+$) is predicted to be accompanied

by a side band ($K^P = 2^+$) of similar moment of inertia, both having essentially $0\hbar\omega$ structure. The $E2$ transition pattern is more consistent with triaxial structure than with axially symmetric rotation. Then, a low-lying $K^P = 0^+$ excited band, with much larger moment of inertia, although only experimentally observed through $J = 4$, is expected to extend to higher angular momentum. This band, in contrast, has something akin to $2\hbar\omega$ structure, and its greater deformation arises primarily from the neutrons.

Acknowledgements

This material is based upon work supported by the U.S. Department of Energy, Office of Science, under Award Numbers DE-FG02-95ER-40934, DESC00018223 (SciDAC4/NUCLEI), and DE-FG02-87ER40371, and by the U.S. National Science Foundation under Award Number NSF-PHY05-52843. TRIUMF receives federal funding via a contribution agreement with the National Research Council of Canada. This research used computational resources of the University of Notre Dame Center for Research Computing and of the National Energy Research Scientific Computing Center (NERSC), a U.S. Department of Energy, Office of Science, user facility supported under Contract DE-AC02-05CH11231.

References

[1] S.C. Pieper, R.B. Wiringa, and J. Carlson (2004) *Phys. Rev. C* **70** 054325.
[2] T. Neff and H. Feldmeier (2004) *Nucl. Phys. A* **738** 357.
[3] P. Maris (2012) *J. Phys. Conf. Ser.* **402** 012031.
[4] C. Romero-Redondo, S. Quaglioni, P. Navrátil, and G. Hupin (2016) *Phys. Rev. Lett.* **117** 222501.
[5] P. Navrátil, S. Quaglioni, G. Hupin, C. Romero-Redondo, and A. Calci (2016) *Physica Scripta* **91** 053002.
[6] M.A. Caprio, P. Maris, and J.P. Vary (2013) *Phys. Lett. B* **719** 179.
[7] P. Maris, M.A. Caprio, and J.P. Vary (2015) *Phys. Rev. C* **91** 014310.
[8] M.A. Caprio, P. Maris, J.P. Vary, and R. Smith (2015) *Int. J. Mod. Phys. E* **24** 1541002.
[9] T. Dytrych, K.D. Sviratcheva, C. Bahri, J.P. Draayer, and J.P. Vary (2007) *Phys. Rev. Lett.* **98** 162503.
[10] T. Dytrych, K.D. Launey, J.P. Draayer, P. Maris, J.P. Vary, E. Saule, U. Catalyurek, M. Sosonkina, D. Langr, and M.A. Caprio (2013) *Phys. Rev. Lett.* **111** 252501.
[11] C.W. Johnson (2015) *Phys. Rev. C* **91** 034313.
[12] M.A. Caprio, P.J. Fasano, P. Maris, A.E. McCoy, and J.P. Vary (submitted) *Eur. Phys. J. A*; arXiv:1912.00083 [nucl-th].
[13] B.R. Barrett, P. Navrátil, and J.P. Vary (2013) *Prog. Part. Nucl. Phys.* **69** 131.
[14] A.M. Shirokov, I.J. Shin, Y. Kim, M. Sosonkina, P. Maris, and J.P. Vary (2016) *Phys. Lett. B* **761** 87.

[15] M. Freer (2007) *Rep. Prog. Phys.* **70** 2149.
[16] Y. Kanada-En'yo, M. Kimura, and A. Ono (2012) *Prog. Exp. Theor. Phys.* **2012** 01A202.
[17] M. Freer, E. Casarejos, L. Achouri, C. Angulo, N.I. Ashwood, N. Curtis, P. Demaret, C. Harlin, B. Laurent, M. Milin, N.A. Orr, D. Price, R. Raabe, N. Soić, and V.A. Ziman (2006) *Phys. Rev. Lett.* **96** 042501.
[18] H.G. Bohlen, T. Dorsch, Tz. Kokalova, W. von Oertzen, Ch. Schulz, and C. Wheldon (2007) *Phys. Rev. C* **75** 054604.
[19] D. Suzuki, A. Shore, W. Mittig, J.J. Kolata, D. Bazin, M. Ford, T. Ahn, D. Becchetti, S. Beceiro Novo, D. Ben Ali, B. Bucher, J. Browne, X. Fang, M. Febbraro, A. Fritsch, E. Galyaev, A.M. Howard, N. Keeley, W.G. Lynch, M. Ojaruega, A.L. Roberts, and X.D. Tang (2013) *Phys. Rev. C* **87** 054301.
[20] D.R. Tilley, J.H. Kelley, J.L. Godwin, D.J. Millener, J.E. Purcell, C.G. Sheu, and H.R. Weller (2004) *Nucl. Phys. A* **745** 155.
[21] D.J. Rowe (2010) "*Nuclear Collective Motion: Models and Theory*". World Scientific, Singapore.
[22] Y. Kanada-En'yo and H. Horiuchi (1997) *Phys. Rev. C* **55** 2860.
[23] Y. Kanada-En'yo, H. Horiuchi, and A. Doté (1999) *Phys. Rev. C* **60** 064304.
[24] T. Suhara and Y. Kanada-En'yo (2010) *Prog. Theor. Phys.* **123** 303.
[25] A.S. Davydov and G.F. Filippov (1958) *Nucl. Phys.* **8** 237.
[26] J. Meyer-ter-Vehn (1975) *Nucl. Phys. A* **249** 111.
[27] D.R. Entem and R. Machleidt (2003) *Phys. Rev. C* **68** 041001.
[28] P. Maris, M. Sosonkina, J.P. Vary, E. Ng, and C. Yang (2010) *Procedia Comput. Sci.* **1** 97.
[29] H.M. Aktulga, C. Yang, E.G. Ng, P. Maris, and J.P. Vary (2013) *Concurrency Computat.: Pract. Exper.* **26** 2631.
[30] M. Shao, H.M. Aktulga, C. Yang, E.G. Ng, P. Maris, and J.P. Vary (2018) *Comput. Phys. Commun.* **222** 1.
[31] M.A. Caprio, P.J. Fasano, J.P. Vary, P. Maris, and J. Hartley (in press) In: A.M. Shirokov and A.I. Mazur (eds) "*Proceedings of the International Conference Nuclear Theory in the Supercomputing Era 2018*". Pacific National University, Khabarovsk, Russia; arXiv:1909.13417 [nucl-th].
[32] G. Alaga, K. Alder, A. Bohr, and B.R. Mottelson (1955) *Mat. Fys. Medd. Dan. Vid. Selsk.* **29**(9).
[33] D.R. Bès (1959) *Nucl. Phys.* **10** 373.
[34] M.A. Caprio and F. Iachello (2005) *Ann. Phys. (N.Y.)* **318** 454.
[35] E. Caurier, P. Navrátil, W.E.Ormand, and J.P. Vary (2002) *Phys. Rev. C* **66** 024314.